MODELLING THE FAR-FIELD ACOUSTIC EMISSION OF ROTATING TURBULENCE

Fabien Godeferd, Claude Cambon, Benjamin Favier
Laboratoire de Mécanique des Fluides et d'Acoustique,
Ecole Centrale de Lyon,
36, avenue Guy de Collongue, 69134 Ecully cedex, France
benjamin.favier@ec-lyon.fr

ABSTRACT

This paper focuses on the acoustic emission of unsteady and anisotropic homogeneous turbulence. A computationally efficient method is introduced in order to model turbulence submitted to rotation. The model for the fluctuations mixes random Fourier modes and inertial waves with variable respective intensities. The acoustic analogy introduced by Lighthill is applied to these sources to estimate the acoustic properties of the incompressible anisotropic field. The modifications induced by rotation on the spectrum of acoustic intensity are discussed. We present results for the acoustic spectrum, sound directivity, and we compare with some theoretical laws.

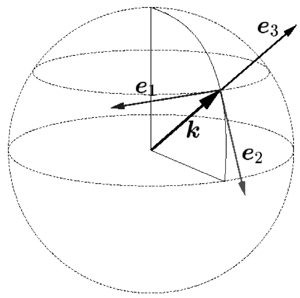

Figure 1: The local Craya-Herring frame

INTRODUCTION

This paper deals with two strongly linked issues of fluid mechanics. We attempt to estimate the far-field acoustic emission of anisotropic turbulence. The omnipresent acoustic issue in industrial situations is far from the academic case of isotropic turbulence. Understanding the phenomena responsible for the non-isotropy of the turbulence, and their consequences in terms of acoustic emission, is an important question in modern aeroacoustics.
The resolution of the complete set of compressible Navier-Stokes equations is still nowadays a very hard numerical task. The acoustic analogy is, in this framework, very helpful. We consider an infinite fluid domain which is locally turbulent and considered as an acoustic source radiating in the medium otherwise at rest. The source field is a turbulent flow of an incompressible fluid without internal acoustic propagation. Using the acoustic analogy applied to these sources, the far field acoustic propagation is then computed. The model used is based on Lighthill's theory, which is, in its first formulation, rigorously exact. However, an accurate estimation of the two-points two-times correlations is required. In our case, a Kinematic Simulation (KS) provides very good correlations compared to the ones coming from Direct Numerical Simulation (DNS). The only hypotheses used here are the far-field approximation and the fact that the acoustic sources are supposed to be compact.
We aim at understanding the consequences on the acoustic field of the restructuration of turbulence submitted to rotation. The model has a low numerical cost, using random Fourier modes and in which no equations is solved. The fixed energy spectrum provides one-time two-points correlations frozen and unchanged by rotation in the linear approximation. However, the unsteady two-times statistics are altered. KS was already used for Lagrangian diffusion (Liechtenstein, 2005) or for acoustic interaction with a mean flow (Béchara, 1994). The first two parts in the following are devoted to the modelisation of a turbulent field submitted to rotation. Lighthill's acoustic analogy will be presented, and followed by the different results obtained thus far.

INERTIAL WAVES IN ROTATING FLUIDS

We study the effect of the rotation on an isotropic and homogeneous turbulence. In a first level of approximation, we will not consider the non-linear restructuration of the flow nor the evolution of the energy spectrum. Coherent eddy structures in rotating flows are not account for, since linear dynamics give access to waves only. By means of an acoustic investigation, we attempt to understand the effects of rotation on the model.
In this part, the anisotropic dispersion relation of the inertial waves existing in a rotating flow is presented. The starting point is the Navier-Stokes equations for an incompressible fluid written in a frame rotating at a rate Ω around an axis assumed to be $\mathbf{n}$:

$$\frac{\partial \mathbf{u}}{\partial t} + (\mathbf{u}\cdot\nabla)\,\mathbf{u} + 2\Omega\mathbf{n}\times\mathbf{u} = -\frac{1}{\rho}\nabla p + \nu\Delta\mathbf{u} \tag{1}$$

$$\nabla\cdot\mathbf{u} = 0 \tag{2}$$

One can write the velocity Fourier components $\hat{\mathbf{u}}(\mathbf{k}) = \left(\hat{u}^{(1)}, \hat{u}^{(2)}, \hat{u}^{(3)}\right)$ (for more details, see Cambon, 2001) in a local orthonormal reference frame in Fourier space (the Craya-Herring frame, see figure 1):

$$\mathbf{e}_1 = \frac{\mathbf{k}\times\mathbf{n}}{|\mathbf{k}\times\mathbf{n}|},\ \mathbf{e}_2 = \frac{\mathbf{k}}{k}\times\mathbf{e}_1,\ \mathbf{e}_3 = \frac{\mathbf{k}}{k} \tag{3}$$

The divergence-free condition (2) imposes $\hat{\mathbf{u}}(\mathbf{k})\cdot\mathbf{k} = 0$, so that the third component of the velocity is useless. An initial velocity field $\mathbf{u}\,(\mathbf{x}, t=0)$ is sufficient to determine the general non viscous linear solution:

$$\mathbf{u}(\mathbf{x},t) = \int \sum_{\epsilon=\pm 1} \mathbf{N}^{\epsilon} e^{-i\epsilon\sigma t}\left(\mathbf{N}^{-\epsilon}\cdot\hat{\mathbf{u}}(\mathbf{k},t=0)\right) e^{i\mathbf{k}\cdot\mathbf{x}} d^3\mathbf{k} \tag{4}$$

where $\mathbf{N}^{\epsilon}$ are the eigenmodes of the linear operator coming from the linearized form of equation (1). One can emphasize the oscillating solutions ($\epsilon = \pm 1$) representing the inertio-gravity waves, whose dispersion relation is:

$$\sigma = 2\Omega \frac{\mathbf{k} \cdot \mathbf{n}}{k} = 2\Omega \cos\theta_n \tag{5}$$

where θ_n is the propagation angle with respect to the rotation axis $\mathbf{n}$, assumed to be vertical. This linearized approach provides a direct relation between a wave number and its time dependence.

KINEMATIC SIMULATION

The scale disparity existing in an incompressible turbulent flow, from acoustic waves to hydrodynamic fluctuations, makes its numerical simulation a hard task. Within the framework of acoustic emission, the calculation of turbulent fluctuations depends on an efficient evaluation of their time and space scales. KS provides an Eulerian velocity field, with good two-points and two-times correlations, without the numerical cost of DNS. The spatial velocity field is synthesized with a method devised by Kraichnan (1970). KS was then used by Karweit (1988) for the propagation of acoustic waves and by Fung (1992) in the case of homogeneous and isotropic turbulence. The noise modelling of free turbulent flows has also been investigated using a stochastic approach, e.g. Béchara (1994).
At any time *t* and at any point $\mathbf{x}$ of the domain,

$$u_i(\mathbf{x}, t) = \Re \sum_{n=1}^{N} e^{i(\mathbf{k}_n.\mathbf{x}+\omega_n t)} \times \left(u^{(1)}(\mathbf{k}_n, t) e_i(\mathbf{k}_n) + u^{(2)}(\mathbf{k}_n, t) e_i(\mathbf{k}_n)\right) \tag{6}$$

The disparity of length scales existing in turbulence must be taken into account using many degrees of freedom, such as $N = 10^3$. The different wave numbers $\mathbf{k}_n$ are chosen according to a random process. The unsteadiness, conveyed by the terms $u^{(1)}(\mathbf{k}_n, t)$ and $u^{(2)}(\mathbf{k}_n, t)$, is given by a discretization of the linear solution (4):

$$\hat{\mathbf{v}}(\mathbf{k}_n, t) \equiv \left(u^{(1)}(\mathbf{k}_n, t), u^{(2)}(\mathbf{k}_n, t)\right) \tag{7}$$

$$= \sum_{\epsilon=\pm 1} \mathbf{N}_n^{\epsilon} e^{-i\epsilon\sigma_n t} \left(\mathbf{N}_n^{-\epsilon} \cdot \hat{\mathbf{v}}(\mathbf{k}_n, 0)\right) \tag{8}$$

Two terms are responsible for the unsteadiness of the flow. The angular frequency ω_n is equivalent to a random phase of translation: all the Fourier modes components are influenced (see equation (6)). σ_n can be considered as rotational random phases.
This model of the velocity field was used in the study of lagrangian diffusion with very good results. Liechtenstein (2005) has shown that the non-linear behaviour of one-particle vertical dispersion in a rotating turbulent flow can be partly predicted by a linear approximation provided that the dispersion relation of the inertio-gravity waves is explicitly used. In the classical method, the unsteadiness was introduced by a dimensional argument. One can link ω_n to the amount of turbulent energy as:

$$\omega_n = \sqrt{k_n^3 E(\mathbf{k}_n)} \tag{9}$$

The angular frequency ω_n is then proportionnal to the eddy turnover time of the *n*th wave mode . Since we are interested in acoustics, the unsteadiness controlling the turbulent domain is essential, and a merely random process cannot take into account the modifications induced by rotation. The inertial waves, and in particular their dispersion relations, are clearly a relevant phenomenon to describe our flow. To the random components coming from (9), we add the deterministic dispersion relation, so that $\sigma_n = 2\Omega\cos\theta_n$ (see equations (5) and (8)) and we use $\omega_n = \lambda\sqrt{k_n^3 E(\mathbf{k}_n)}$, where λ controls the amount of random angular pulsations in the global unsteasiness. Thus, we relate the time evolution of one Fourier mode to the rate of rotation, and to its orientation. However, in the present model, KS does not take into account the fact that the motion of the finest scales of the flow is modified by the larger ones, the so-called sweeping effect, rediscussed at the end.

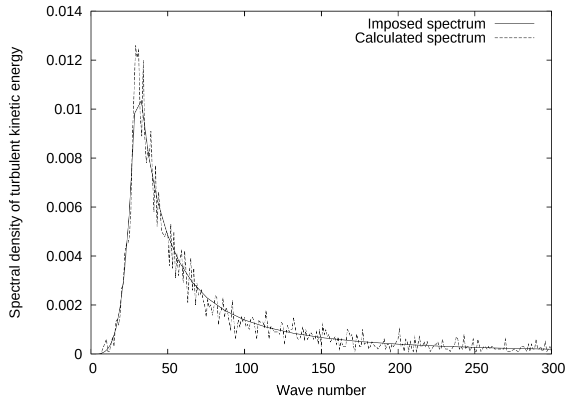

Figure 2: Comparison between the analytic turbulent energy spectrum and the calculated one with 1000 Fourier modes.

Finally, the amplitudes of the N different modes are determined by a turbulent energy spectrum, which is, in first approach, supposed to be isotropic (figure 2). We however introduce a new feature: the original method generates one random direction for each wave number in the discrete range $[k_{\min}, k_{\max}]$, which is consistent in isotropic cases. In our model, even the modulus of the wave number is a random variable, which is more relevant to the anisotropic case.

LIGHTHILL'S ANALOGY

In 1952, Lighthill published his famous paper about the acoustic analogy, which was one of the first attempts to predict the noise generated by turbulence. He has shown that the instantaneous acoustic pressure is strongly linked to the instantaneous velocity field. By rearranging the Navier-Stokes equation, Lighthill established the following equation:

$$\frac{\partial^2 \rho}{\partial t^2} - c_0^2 \frac{\partial^2 \rho}{\partial {y_j}^2} = \frac{\partial^2 T_{ij}}{\partial y_i \partial y_j} \tag{10}$$

in which ρ is the fluctuating fluid density and c_0 the velocity of sound. Lighthill's tensor is defined by

$$T_{ij} = \rho_0 u_i u_j + (p' - \rho_0 {c_0}^2)\delta_{ij} - \tau_{ij} \tag{11}$$

This tensor is the result of three contributions: a convective nonlinear unsteadiness $\rho_0 u_i u_j$, the noise known as "entropy noise" (negligible in our case) and the viscous stress fluctuations τ_{ij}, neglected most of the time.
Implicitly, Lighthill's analogy assimilates the acoustic emission of turbulence to a volumic unsteady source, resulting from the action of external forces $\frac{\partial^2 T_{ij}}{\partial y_i \partial y_j}$. Under classical hypotheses of far-field and statistical stationnarity, a solution of Lighthill's formalism can be obtained by means of Green's functions. For an external observer located at the point $\mathbf{x}$, the fluctuating pressure is given by:

$$p(\mathbf{x}, t) = \frac{1}{4\pi {c_0}^2} \frac{x_i x_j}{x^3} \int_V \frac{\partial^2}{\partial t^2} T_{ij}\left(\mathbf{y}, t - \frac{|\mathbf{x} - \mathbf{y}|}{c_0}\right) d^3\mathbf{y} \tag{12}$$

where V is the volume of the turbulent domain. One can take the time Fourier transform of equation (12):

$$\tilde{p}(\mathbf{x}, \omega) = \frac{\omega^2}{4\pi {c_0}^2} \frac{x_i x_j}{x^3} \int_V \tilde{T}_{ij}(\mathbf{y}, \omega)\, e^{j\omega \frac{|\mathbf{x}-\mathbf{y}|}{c_0}} d^3\mathbf{y} \tag{13}$$

where $\tilde{p}(\mathbf{x}, \omega)$ and $\tilde{T}_{ij}(\mathbf{y}, \omega)$ are respectively the time Fourier transforms of $p(\mathbf{x}, t)$ and $T_{ij}(\mathbf{y}, t)$. The acoustic intensity, proportional

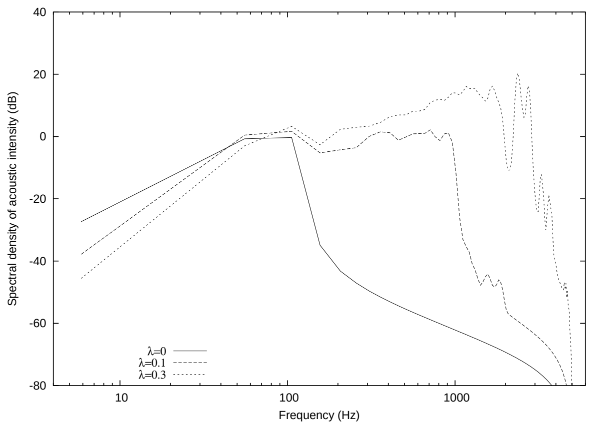

Figure 3: Spectral density of acoustic energy $I(f)$. The rotation rate is fixed at 32π rad.s^{-1}. The random unsteadiness, via the parameter λ, is progressively introduced. In order to make the visualisation easier, the spectra are smoothed.

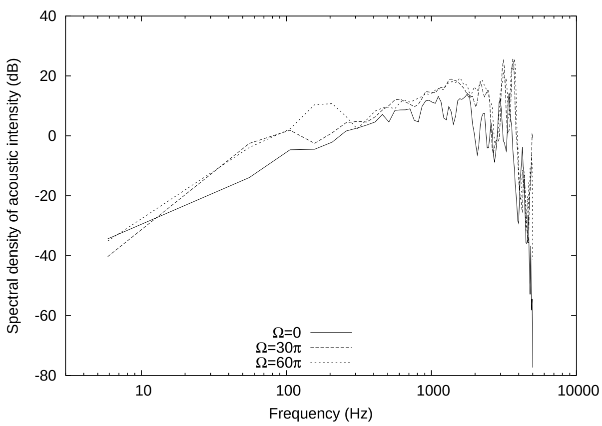

Figure 4: Spectral density of acoustic energy with different rates of rotation.

to the autocorrelation function of $p(\mathbf{x}, t)$, is, in our case, obtained in Fourier space:

$$I(\omega) = \frac{\tilde{p}(\mathbf{x}, \omega)\tilde{p}^*(\mathbf{x}, \omega)}{\rho_0 c_0} \tag{14}$$

where $\tilde{p}^*(\mathbf{x}, \omega)$ is the complex conjugate of $\tilde{p}(\mathbf{x}, \omega)$. As emphasized by Witkowska (1994), Lighthill's problem is slightly different from ours. Indeed, the original point of view was to observe an infinite fluid domain in which only a small part is turbulent. The numerical simulations performed in this paper concern only a fraction of the turbulent domain observed by Lighthill. The surfaces delimiting the field can take part in the global acoustic emission. The formulation used here avoids such artifical contributions, although it is not the case of all acoustic analogies.

RESULTS

Kinematic Simulation, in which the unsteadiness comes from the dispersion relation of inertial waves, provides the turbulent field required to compute the Lighthill's analogy. In the following, we discuss different results coming from this approach.
The different parameters likely to modify the acoustic spectrum are:

- the parameter λ representing the contribution of the random pulsations to the global instationarity. λ cannot be larger than $\mathcal{O}(1)$ whereas $\lambda = 0$ corresponds to a frozen field without rotation (Fung, 1998). In our calculations, λ is chosen equal to 0.4.
- the rotation rate Ω, which is directly linked with the *global Mach number* defined by $M_0 = \frac{\Omega L}{c_0}$, where L is a characteristic length of the physical domain.
- the root mean square velocity q, which defines the *local Mach number* defined by $m_0 = \frac{q}{c_0}$

The ratio m_0/M_0 is the Rossby number of the flow.

Acoustic spectra

We present here the spectral density of acoustic energy $I(f)$. In order to access the high-frequency noise, the time step is equal to 10^{-4} s. This ensures a maximum frequency about 5000 Hz. On the other hand, the number of time steps must be adequate to have a sufficient observation time. Indeed, our version of Lighthill's theory takes into account the retarded time between two different points of the source. The acoustic emission starts at $t = 0$, the first perturbation felt by the observer will be at $t_r = r/c_0$. We must observe the acoustic source during a time much longer than t_r. In our case, $t_r \approx 0.03$ s, and 4096 steps in time are sufficient. The field is synthesized in a cube of side 0.5 m with a resolution from 12^3 to 32^3 depending on the calculation.
First, figure 3 presents the spectrum of the rotating turbulence, without random angular frequency (i.e. $\lambda = 0$). There appears a cut-off frequency coming from the maximum pulsation of the inertial waves. Given that the acoustic intensity is proportional to the velocity squared, whose maximum angular frequency σ_{max} is 2Ω rad.s^{-1}, we expect to observe a cut-off at $\sigma_{\text{max}} = 4\Omega$ rad.s^{-1}. In our case, the spectra are computed for a rotation rate of 36π rad.s^{-1}, so that $f_{\text{max}} = \sigma_{\text{max}}/2\pi \approx 72$ Hz. The two other curves in figure 3 present the same calculation with $\lambda \neq 0$. The unsteadiness of the synthesized field is then enhanced and some high-frequency components appear.
Figure 4 shows how the rotation rate influences the spectrum. Background rotation impacts mainly for a frequency domain influenced by inertial waves, from 0 to $2\Omega/\pi$ Hz. Again, we observe the cut-off depending on the rotation rate, but this contribution is superposed to the one due to the random unsteadiness. The integral obtained thanks to Lighthill's theory shows that the intensity varies like the pulsation at the power of four. A comparison of our results is possible with a DNS approach. Indeed, a similar domain of turbulent flow can be solved using a pseudo-spectral code of DNS. Applying the same acoustic analogy to this solution, it is possible to obtain the same acoustic spectra. As already observed (see for example Sarkar (1993) or Witkowska (1994)), the time scale of the structures that have the maximum acoustic emission is greater than the time scale of the energetic structures of the turbulence. One can define a time scale for those structures as l_0/u_0 where l_0 is the integral scale and u_0 a characteristic velocity. In our case, $l = 0.03$ m whereas $u = 10$ m.s^{-1}. Thus, the Strouhal number $St = fl_0/u_0$ of the structures which have the maximum acoustic emission is $St \approx 4 - 6$.

Dependence on local Mach number

One of the most impressive results from Lighthill's theory is the dependence of the acoustic power with the local Mach number. Under the far-field hypothesis, the acoustic intensity can be dimensionally estimated by:

$$\overline{I} \approx \rho_0 \left(\frac{D}{4\pi|\mathbf{x}|}\right)^2 {u'_0}^3 {M_0}^5 \tag{15}$$

In other terms, the acoustic intensity is proportional to the Mach num-

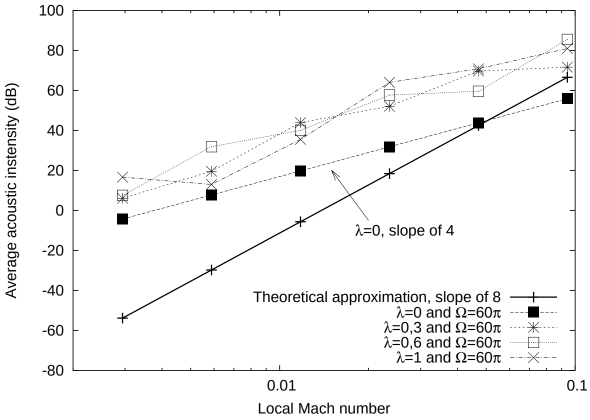

Figure 5: Evolution of the acoustic intensity depending on the local Mach number. The random pulsation increases progressively

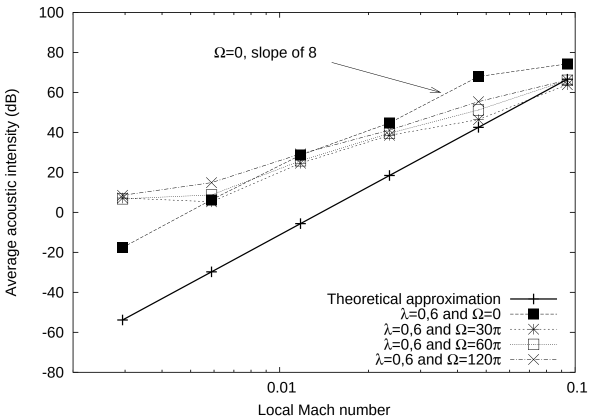

Figure 6: Evolution of the acoustic intensity depending on the local Mach number. The rate of rotation increases progressively

ber of the flow at the power of eight. An interesting question is to chek wether our model follows this dependence, and the impact of rotation. We compute the intensity at a given point for different values of the root mean squared velocity, that is for different local Mach numbers $m_0 = q/c_0$, and for different values of λ and Ω. We study the influence of these parameters, characterizing the unsteadiness, on the acoustic emission. Figure 5 shows the progressive increase of λ, whereas Ω is maintained constant. When $\lambda = 0$, the acoustic intensity varies like the Mach number at the power four. The turbulence seems to follow a monopolar behaviour, whereas Lighthill's theory predicts a quadrupolar one. However, this result can be understood by writing Lighthill's tensor, in an absolute reference frame (equations (1)-(2) were obtained in a rotating frame):

$$\begin{aligned} T_{ij} &= \rho_0[(u_i + (\mathbf{\Omega} \times \mathbf{x})_i)(u_j + (\mathbf{\Omega} \times \mathbf{x})_j)] \\ &= \rho_0[(u_i - x_j\Omega)(u_j + x_i\Omega)] \\ &= \rho_0[(u_iu_j + x_iu_i\Omega - x_ju_j\Omega - x_ix_j\Omega^2] \end{aligned} \tag{16}$$

in which $\mathbf{x}$ is the current point of calculation of the Lighthill's tensor and Ω the amplitude of rotation (i.e. the vertical component). When $\lambda = 0$, the flow is dominated by rotation, which implies that the Rossby number is low, $u_i \ll \Omega x$. Only the last term of equation (16) is not negligible. We finally have $T_{ij} \approx \rho_0 x_i x_j \Omega^2$. The volumic

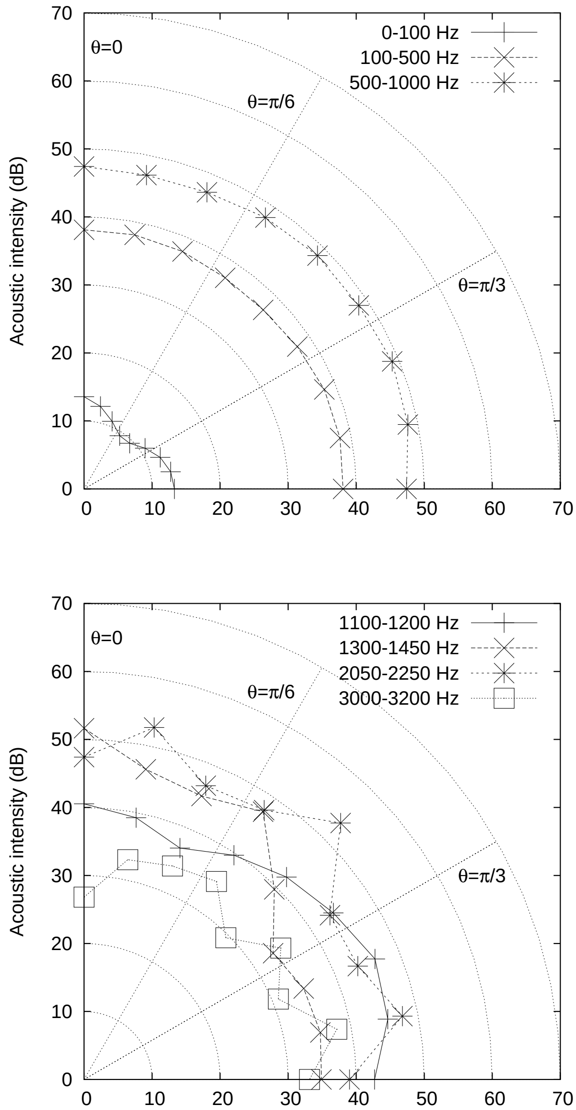

Figure 7: Directivity of the acoustic emission depending on the frequency for the case without rotation. Two frequency bands having a similar behaviour are gathered. Only the frequency bands of interest are presented. The acoustic intensity is shown in decibels.

unsteady source of acoustic emission is then:

$$\frac{\partial^2 T_{ij}}{\partial x_i \partial x_j} \approx \rho\Omega^2 \tag{17}$$

This term does not display any explicit space dependence, a characteristic of an acoustic monopole.

However, when adding some random pulsation by increasing λ (and so by increasing the Rossby number), the behaviour of the synthesized turbulence should be a quadrupolar one. Our results show that the random pulsations disturb the monopolar law in power four and, on some range of Mach number, Lighthill's law appears.

These conclusions are confirmed by the results presented in figure 6: a pure random unsteadiness altered by rotation. As predicted, the isotropic case $\Omega = 0$ rad.s^{-1} follows the dependence in the power eight. Depending on the Rossby number, the acoustic emission of the turbulent domain will result in the transition from monopolar (strong rotation) to quadrupolar behaviour (isotropic turbulence).

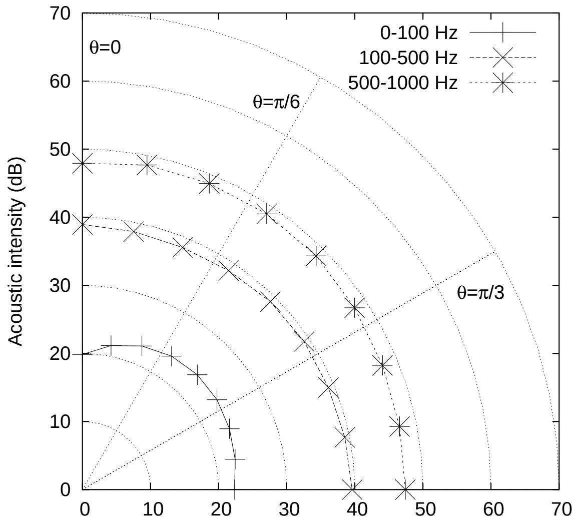

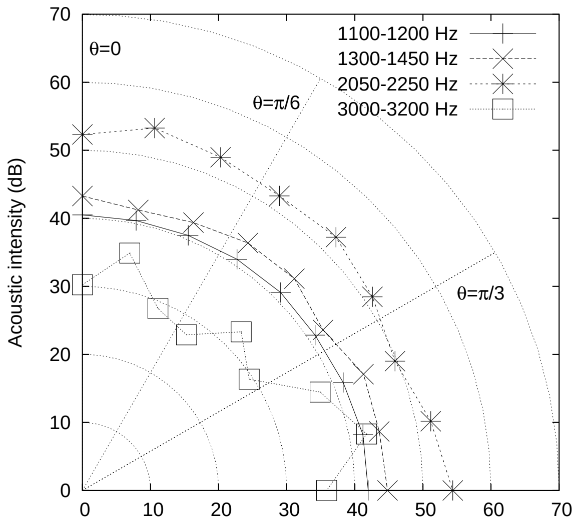

Figure 8: Directivity of the acoustic emission depending on the frequency for a rotation rate $\Omega = 60\pi$ rad.s^{-1}.

An other characterization of this behaviour would be to compute the two contributions of the acoustic pressure independently. The symmetrical tensor $\ddot{T}_{ij}$ of equation (11), can be recast as:

$$\ddot{T}_{ij} = \left(\ddot{T}_{ij} - \frac{1}{3}\ddot{T}_{ll}\delta_{ij}\right) + \frac{1}{3}\ddot{T}_{ll}\delta_{ij} = Q_{ij} + Q\delta_{ij} \qquad (18)$$

where Q_{ij} is a zero-trace tensor and Q a scalar. Then, the acoustic pressure at the retarded time τ can be split as a sum of two terms, which respectively represent the contribution from monopole and quadrupole sources:

$$p(\mathbf{x}, t) = \frac{1}{4\pi {c_0}^2}\left(\int_V Q(\mathbf{y}, \tau)\, d\mathbf{y} + n_i n_j \int_V Q_{ij}(\mathbf{y}, \tau)\, d\mathbf{y}\right)$$

Directivity

Regarding the spectral distribution, the isotropy of homogeneous turbulence can be broken when the flow is submitted to background rotation. In a first approximation, KS model used here is based on an isotropic energy spectrum. Further developments will introduce an anisotropic spectrum. However, an anisotropic directivity of the sound emitted by rotating turbulence may come from the inertial waves anisotropic dispersion relation. In this part, we present some of the acoustic properties of the source field depending on the position of the observer. Given the symmetry of the flow, we have computed only a quadrant from $\theta = 0$ to $\theta = \pi/2$. All the preceding results were computed with $\theta = \pi/4$. Two configurations are observed: with and without background rotation, in order to constrast with the isotropic case.

To investigate the behaviour of KS in terms of directivity, the acoustic intensity $\overline{I}_n(\mathbf{x})$ for different positions $\mathbf{x}$ of the observer is calculated by partial integrations of the spectral density of acoustic intensity:

$$\overline{I}_n(\mathbf{x}) = \int_{f_n}^{f_{n+1}} I(f)df \qquad (19)$$

with $f_{n+1} - f_n \approx 100$ Hz. Different bands $[f_n, f_{n+1}]$ of similar behaviour are then gathered in the same curve.

Various behaviours can be highlighted looking at figure 7. First, the very low frequencies, from 0 to 100 Hz, are quite anisotropic. Then, a large spectral band, from 100 to $1000 - 1200$ Hz, is isotropic. As the frequency increases, the isotropy is gradually lost. For clarity, we have chosen to present only some spectral bands.

Figure 8 presents the same results with a strong rotation rate $\Omega = 60\pi$ rad.s^{-1}. In this case, almost all the frequencies approach an isotropic behaviour. In particular, the very low frequencies, in which the inertial waves are dominant, are influenced by the effect of rotation. This suggests that the synthesized field is dominating by its monopolar properties, as emphasized in the preceding paragraph.

Proudman's theory

Until now, we have observed the qualitative anisotropic features of our model in terms of spectral density and directivity. We now attempt to present quantitative results in terms of acoustic power. KS is a statistically steady model of turbulence, producing a constant average acoustic power during the time evolution of the source. However, after Lighthill's paper, Proudman (1952) calculated the acoustic power of turbulence as a function of the turbulent energy spectrum. This theory is based on the hypothesis of isotropic homogeneous turbulence, and we expect to observe differences at increasing rotation rate. The acoustic power is given by:

$$P_{\text{Proudman}} = \alpha_p \frac{q^3}{L} m^5 \qquad (20)$$

where α_p depends on the energy spectrum. Following Proudman's reasoning, the α_p coefficient of our spectra is about 13. This is close to the value found by Witkowska (1994) with a DNS approach. This value is compared to the one obtained by the direct computation of the acoustic power P_{num}:

$$\alpha_n = \frac{P_{\text{num}}}{\frac{q^3}{L} m_0^5} \qquad (21)$$

In order to estimate the acoustic power, we have computed the acoustic intensity averaged over ten different observation points. The results depending on the rate of rotation are gathered in the table 1. It

Ω	α_n	α_p
0	3.56	13
30π	2.17	13
60π	1.55	13

Table 1: Comparison with the Proudman's theory

seems that the acoustic efficiency of the turbulence decreases with the rate of rotation Ω. Moreover, our results are consistent with the DNS and Large Eddy Simulation (LES) approaches by Witkowska (1994), which seems to imply that Proudman's theory overestimates the acoustic emission.
The quantitative behaviour of the KS in terms of acoustic emission seems to be acceptable, especially looking at numerical costs.

CONCLUSION AND PERSPECTIVES

Lighthill's acoustic analogy and a stochastic modelisation of a bounded turbulent domain allow us to estimate the acoustic properties of rotating homogeneous turbulence. The isotropy of the flow is broken by the inertial waves whose dispersion relation is explicitly used. Their influence on the acoustic emission is dominant for low frequencies below $2\Omega/\pi$ Hz. The maximum of the acoustic emission concerns pulsations greater than the pulsation characteristic of the most energetic structure. However, this result, already observed by DNS or LES approaches, shows a strong dependence with the parameter λ. Looking at the dependence of acoustic emission with the local Mach number and its directivity, we have separated the monopolar behaviour of the stochastic field from the quadrupolar one. Finally, our calculations are consistent with previous comparisons of Proudman's theory with DNS ans LES calculations.
Beyond those results, many elements of the KS could be improved. The energy spectrum used in KS could be refined to include a dependence on the direction of the wave number. Moreover, the different behaviours observed, in terms of directivity for example, must be compared with the ones coming from a DNS calculation. This aspect of the study is still in progress. As emphasized by Fung (1992), the sweeping effect, whereby the fine scales of the turbulence are convected by the larger ones, is not included in this version of the Kinematic Simulation model. An updated version is currently studied with an approach close to Fung's one, in which the larger scales determine the unsteadiness of the smaller ones with ω_n of order $\mathbf{k}_n \cdot \mathbf{u}$. Our results have shown the strong dependence with λ of the acoustic spectrum, and the modelisation of the sweeping effect might be a solution to overcome this issue. Recent works, e.g. Poulain (2006), about dynamics of spatial Fourier modes and temporal intermittency in turbulence could also be of interest to improve the relevancy of our model to the aeroacoustics field.

REFERENCES

Béchara, W., Bailly, C., Lafon, P., Candel, S.M., 1994, "Stochastic approach to noise modeling for free turbulent flows", *AIAA Journal*, Vol. 32, No. 3, pp. 455-463.

Cambon, C., 2001, "Turbulence and vortex structures in rotating and stratified flows", *Eur. J. Mech. B. - Fluids*, 20, pp. 489-510.

Fung, J.C.H., Hunt, J.C.R., Malik, N.A., Perkins,R.J., 1992, "Kinematic simulation of homogeneous turbulence by unsteady random Fourier modes", *J. Fluid Mech.*, Vol. 236, pp. 281-318.

Fung, J.C.H., Vassilicos, J.C., 1998, "Two particles dispersion in turbulent-like flows", *Phys. Rev. E.*, Vol. 57, Number 2, pp. 1677-1690.

Goldstein, M., Rosenbaum, B., 1973, "Effect of anisotropic turbulence on aerodynamic noise", *J. Acoust. Soc. Am.*, Vol. 54, Number 3, pp. 630-645.

Karweit, M., Blanc-Benon, P., Juvé, D., Comte-Bellot, G., 1988, "Simulation of the propagation of an acoustic wave through a turbulent velocity field", 17th International Union of Theoretical and Applied Mechanics, Grenoble, France, pp. 21-27.

Kraichnan, R.H., 1970, "Diffusion by a random velocity field", *The Physics of Fluids*, Vol. 13, No. 1, pp. 22-31.

Liechtenstein, L., Godeferd, F.S., Cambon, C., 2005, "Nonlinear formation of structures in rotating stratified turbulence", *J. of Turb.*, Vol. 6, No. 24.

Lighthill, M., 1952, "On sound generated aerodynamically, I General theory", *Proc. Roy. Soc.*, Vol. A211.

Poulain, C., Mazellier, N., Chevillard, L., Gagne, Y., Baudet, C., 2006, "Dynamics of spatial Fourier modes in turbulence" *Eur. Phys. J. B*, Vol. 53, pp. 219-224.

Proudman, I., 1952, "The generation of noise by isotropic turbulence", *Proc. Roy. Soc. A*, Vol. 214, pp. 119-132.

Witkowska, A., 1994, "Estimation numérique du bruit rayonné par une turbulence isotrope", *Thèse, Ecole Centrale de Lyon*.